Yonago Acta medica 1997;40:117–123

Chondroitin Sulfate Iron Colloid-Enhanced MR Imaging in Patients with Small Hepatocellular Carcinomas: Correlations with Hemodynamic and Pathologic Examinations

Masayuki Kamba, Yuji Suto, Fumiko Kodama, Shuji Sugihara and Kotaro Yoshida

Department of Radiology, Faculty of Medicine, Tottori University, Yonago 683, Japan

To determine the usefulness of chondroitin sulfate iron colloid (CSIC)-enhanced magnetic resonance imaging (MRI) in evaluation of the histologic grade of hepatocellular carcinoma (HCC), we performed a comparative study with computed tomography during arterial portography (CTAP) and CT arteriography. Twenty-one surgically resected HCCs 3 cm or less in diameter were examined. There were five well-differentiated, six well- to moderately-differentiated and ten moderately- or poorly-differentiated HCCs. T2-weighted spin echo images (repetition time: 2,000 ms, echo time: 90 ms) were taken before and after intravenous injection of 23.6 *μmol*Fe/kg of CSIC. The differences between precontrast and postcontrast contrast-to-noise ratios (enhancement index) was correlated with the findings of CTAP, CT arteriography and histological examination. The enhancement index increased with statistical significance as the intranodular arterial perfusion increased ($P < 0.01$), and as the intranodular portal perfusion decreased ($P < 0.01$). Though the enhancement index tended to increase as the grade of malignancy increased, no statistical significance was found. CSIC-enhanced MRI allowed a noninvasive evaluation of the intranodular reticuloendothelial function. We consider this procedure as a supplementary method for evaluation of the histologic grade of HCC prior to performing invasive procedures such as angiography and biopsy.

Key words: computed tomography; contrast enhancement; iron colloid; hepatocellular carcinoma; magnetic resonance imaging

We have used chondroitin sulfate iron colloid (CSIC; Blutal, Dainippon Pharmaceutical Co., Osaka, Japan) as a magnetic resonance (MR) contrast agent to detect hepatocellular carcinoma (HCC) (Kato et al., 1993; Kamba et al., 1994). Intravenous CSIC is rapidly taken up mainly into the reticuloendothelial cells, and consequently it reduces the signal intensity of the liver because of a T2-shortening effect (Kato et al., 1993). CSIC enhances the contrast between liver parenchyma and HCC, where the reticuloendothelial function is impaired or absent in the latter (Kato et al., 1993; Kamba et al., 1994; Suto et al., 1993). This improves the detection of hepatocellular carcinoma (HCC) (Kato et al., 1993; Kamba et al., 1994). A correlation has been found between the enhancement of tumor-liver contrast after CSIC administration and the histologic grade of HCC (Suto et al., 1995; Kamba et al., 1996).

On the other hand, computed tomography during arterial portography (CTAP) and CT arteriography are usually used to evaluate the histologic grade of HCC from the hemodynamic aspect (Matsui et al., 1991; Takayasu et al., 1995). In this study, we compared CSIC-

Abbreviations: C/N, contrast-to-noise ratio; CSIC, chondroitin sulfate iron colloid; CT, computed tomography; CTAP, CT during arterial portography; HCC, hepatocellular carcinoma; MR, magnetic resonance

enhanced MR imaging with CTAP and CT arteriography to confirm the usefulness of CSIC-enhanced MR imaging as a noninvasive method for evaluating the histologic grade of HCC.

Subjects and Methods

CSIC is a stable iron colloid preparation with a trivalent iron ion (Okuhata, 1992). It is used in clinical practice in Japan for treatment of iron deficiency anemia, and its safety has already been established (Kato et al., 1993). It is a paramagnetic substance with a mean molecular weight of 75,000 (Okuhata, 1992). The particle size of this substance is more than 100 nm in water (Okuhata, 1992). Its T1 and T2 relaxivities are 0.44 and 2.3 $s^{-1} \cdot mM^{-1}$, respectively, as measured with a 1.5 T MR spectrometer at 22˚C (Okuhata, 1992).

From January 1991 to June 1994, 26 patients (17 men and 9 women, mean age: 58.7 years) with HCC underwent surgery after CSIC-enhanced MR imaging, CTAP and CT arteriography. Pathological examination disclosed 34 HCCs in the resected specimens. CSIC-enhanced MR imaging revealed 31 HCCs, of which 5 were well-differentiated, 6 well- to moderately-differentiated, and 20 moderately- or poorly-differentiated HCC. The mean diameter was 1.42 cm (range: 1.0–2.0 cm) for the well-differentiated HCCs, 1.57 cm (range: 1.2–2.5 cm) for the well- to moderately-differentiated HCCs, and 4.16 cm (range: 0.9–12.0 cm) for the moderately- or poorly-differentiated HCCs. For this study, the moderately- or poorly-differentiated HCCs of 3 cm or less in diameter (10 nodules, range: 0.9–3.0 cm, mean: 1.95 cm) were selected to match the first two groups in size.

All patients were examined with a Magnetom H15 system with a body coil operating at 1.5 T (Siemens, Erlangen, Germany). Spin echo T2-weighted images (repetition time/echo time 2,000/90 ms, 2 signal excitations) were taken. The slice thickness was 10 mm with a 2-mm gap. The field of view was 370 mm, and the matrix was 160×256. MR images were taken before and 1 h after intravenous injection of 23.6 μmolFe/kg body weight of CSIC. All patients gave written consent to participate in this MR study.

Regions of interest were selected to measure the signal intensity of the lesion and surrounding hepatic parenchyma. The SD of the background noise was measured from a region outside the body along the phase-encoding direction. The contrast-to-noise ratio (C/N) was calculated by dividing the difference in signal intensity between the lesion and liver by the SD of the background noise. The enhancement index was calculated by subtracting the precontrast C/N from the postcontrast C/N.

CTAP and CT arteriography were performed with a Vertex 3000 (Yokogawa Medical Systems, Tokyo, Japan) or a Somatom Plus-S (Siemens). Fifteen or seventeen sequential images of the entire liver were taken with the Vertex 3000 scanner in two or three repeat series of five to eight contiguous scans with a 10-mm slice thickness and 10-mm table increments (scan time: 1.8 s/section). For CTAP, 100 mL of nonionic contrast material [iohexol (Omnipaque; Daiichi Pharmaceutical, Tokyo) or iopamidol (Iopamiron; Nihon Schering, Osaka), 300 mgI/mL] was injected at a rate of 1.0 to 1.3 mL/s via a catheter placed in the superior mesenteric artery. Scanning began 25 to 30 s after starting injection. For CT arteriography,

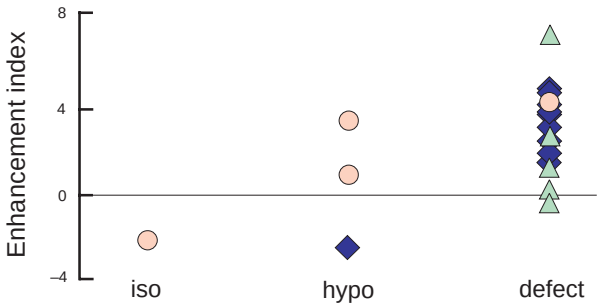

Fig. 1. Relationship between the findings of CTAP and the enhancement index. iso, isoattenuating; hypo, hypoattenuating; ○, well-differentiated HCC; △, well- to moderately-differentiated HCC; ◆, moderately- or poorly-differentiated HCC.

nonionic contrast material (iohexol, 140 mgI/mL) was injected at a rate of 1.2 to 1.5 mL/s during scanning via a catheter placed in the common hepatic or replaced right hepatic artery. Spiral volumetric scan (Kalender et al., 1990) of the whole liver was done by a Somatom Plus-S scanner during a single breathhold (up to 32 s) with a 5-mm slice thickness and table movement of 5 mm/s (scan time: 1 s/section). For CTAP, nonionic contrast material (iohexol, 140 mgI/mL) was injected at a rate of 3 mL/s via a catheter placed in the superior mesenteric artery. Scanning began 30 s after starting injection. For CT arteriography, nonionic contrast material (iohexol, 140 mgI/mL) was injected at a rate of 1.2 to 1.5 mL/s during scanning via a catheter placed in the common hepatic or replaced right hepatic artery.

On CTAP, lesions with attenuation less than the surrounding hepatic parenchyma were classified into two categories: "defect" lesions whose attenuation was less than that of the hepatic portion of the inferior vena cava, and "hypoattenuating" lesions whose attenuation was equal to or greater than that of the hepatic portion of the inferior vena cava. Lesions with attenuation equal to that of the surrounding hepatic parenchyma were described as "isoattenuating."

The enhancement patterns of lesions seen on CT arteriography were classified into three categories according to their attenuation relative to that of the surrounding hepatic parenchyma; hyperattenuating, isoattenuating and hypoattenuating.

The histologic grade of HCC was assessed according to the criteria of the Third Edition of the General Rules for the Clinical and Pathological Study of Primary Liver Cancer by the Liver Cancer Study Group of Japan (The Liver Cancer Study Group of Japan, 1992).

Correlations between the enhancement index and the degree of enhancement on CTAP or CT arteriography, and between the enhancement index and the histologic grade were analyzed by Spearman's rank order test. The level of statistical significance was set at $P < 0.05$.

Results

The relationship between the findings of CSIC-enhanced MR imaging and those of CTAP is summarized in Fig. 1. Seventeen HCCs (nine moderately- or poorly-differentiated, six well- to moderately-differentiated, and two well-differentiated) showed defects on CTAP. The mean enhancement index was 2.98. Sixteen lesions were positive for the enhancement index, whereas one well- to moderately-differentiated HCC was negative. Three HCCs (one moderately- or poorly-differentiated, and two well-differentiated) were hypoattenuating on CTAP. The mean enhancement index was 0.60. Two well-differentiated HCCs were positive for the enhancement index, whereas one moderately- or poorly-differentiated HCC was negative. One well-differentiated HCC was isoattenuating on CTAP, but it was negative for the enhancement index. A statistically significant correlation was found between the enhancement index and portal blood supply demonstrated by CTAP ($rS = 0.575$, $n = 21$, $P < 0.01$).

The relationship between the findings of CSIC-enhanced MR imaging and those of CT arteriography is summarized in Fig. 2. Fourteen HCCs (eight moderately- or poorly-differentiated, four well- to moderately-differentiated, and two well-differentiated) were hyperattenuating on CT arteriography. The mean enhance-

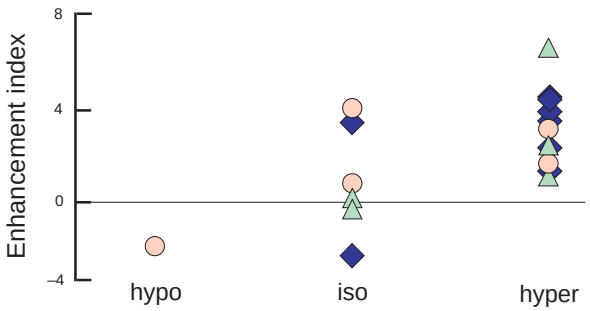

Fig. 2. Relationship between the findings of CT arteriography and the enhancement index. hypo, hypoattenuating; iso, isoattenuating; hyper, hyperattenuating; ○, well-differentiated HCC; △, well- to moderately-differentiated HCC; ◆, moderately- or poorly-differentiated HCC.

Table 1. Relationship between the histologic grade of HCC and the enhancement index

HCC		Enhancement index
Well-differentiated	[5]	1.68 ± 2.53
Well- to moderately-differentiated	[6]	2.28 ± 2.77
Moderately- or poorly-differentiated	[10]	2.82 ± 2.19

Mean ± SD.
[ ], number of lesions.

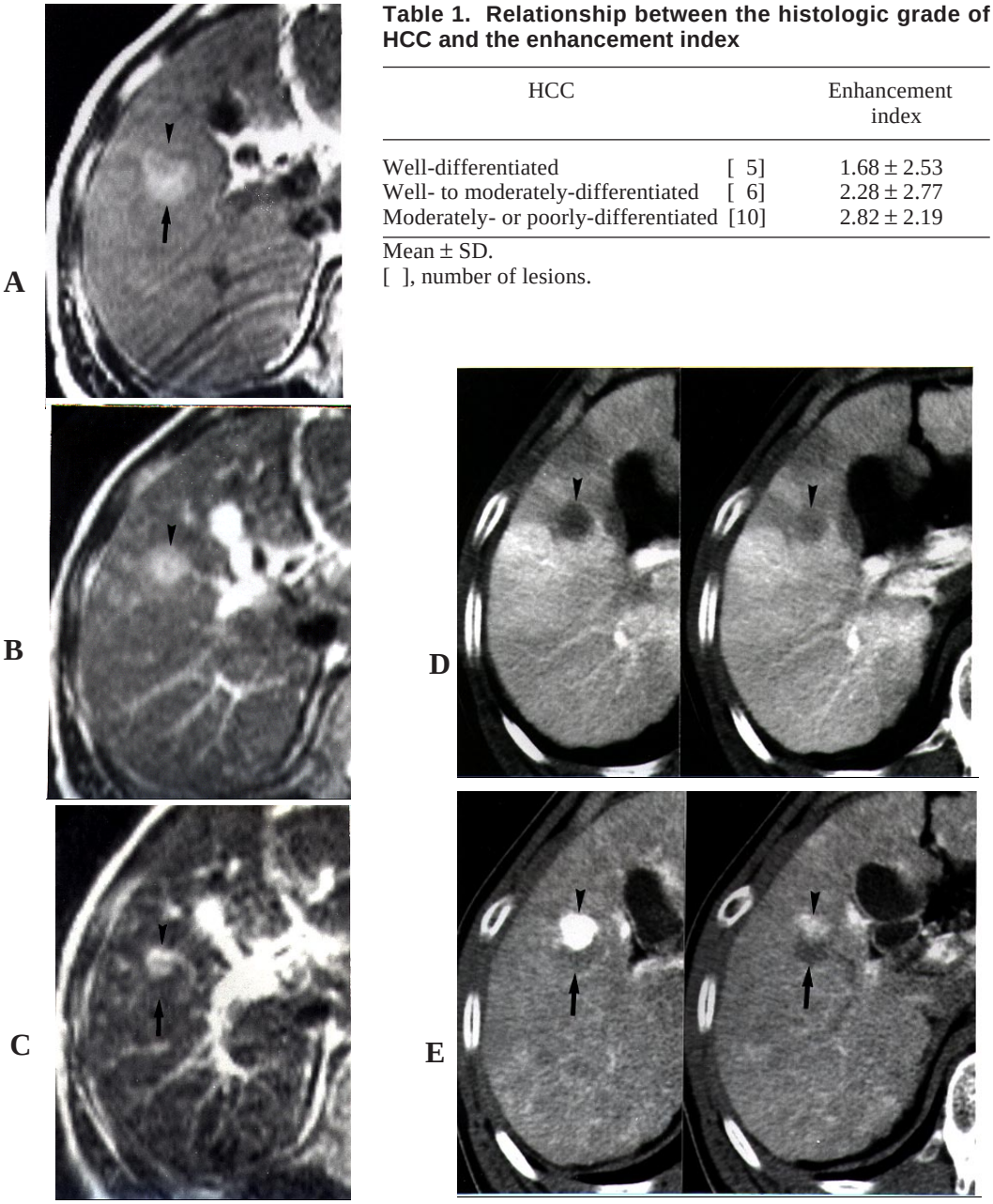

Fig. 3. A 48-year-old man with HCC. **A:** The precontrast T1-weighted image reveals a hyperintense nodule (arrow) with a central isointense component (arrowhead). **B:** The precontrast T2-weighted image shows a central hyperintense component (arrowhead) within a peripheral isointense area. **C:** The central component is enhanced on the CSIC-enhanced T2-weighted image (arrowhead), whereas the peripheral component is slightly hypointense in comparison with the surrounding liver (arrow). **D:** CTAP reveals a portal perfusion defect corresponding to the central component (arrowhead). The peripheral component is isoattenuating. **E:** CT-arteriography shows a central hyperattenuating area (arrowhead) and a peripheral hypoattenuating area (arrow). **F (p. 121):** A photomicrograph of the resected specimen shows a well-differentiated HCC (right half) and a moderately-differentiated HCC (left half). Hematoxylin and eosin stain, ¥ 130. (Figures are reprinted from Kamba et al., 1996)

ment index was 3.30. All the lesions were positive for the enhancement index. Six HCCs (two moderately- or poorly-differentiated, two well- to moderately-differentiated, and two well-differentiated) were isoattenuating on CT arteriography. One well- to moderately-differentiated, and one moderately- or poorly-differentiated HCC were negative for the enhancement index. The mean enhancement index was 1.04. One well-differentiated HCC was hypoattenuating on CT arteriography. The lesion was negative for the enhancement index. A statistically significant correlation was found between the enhancement index and arterial blood supply demonstrated by CT arteriography (rS = 0.577, n = 21, $P < 0.01$).

Though the enhancement index tended to increase as the grade of malignancy increased, no statistically significant correlation was found. Considerable overlap in the enhancement index was observed in the three histologic grades (Table 1).

Representative case

A patient with HCC exhibiting a concentric structure of different histologic grades underwent surgery after CSIC-enhanced MR imaging, CTAP and CT arteriography (Fig. 3). The central component (moderately-differentiated HCC) was enhanced in comparison with the surrounding liver after CSIC injection. The peripheral component (well-differentiated HCC) was not enhanced. CTAP showed a portal perfusion defect corresponding to the central component. The peripheral component was isoattenuating. CT-arteriography showed a central hyperattenuating area and a peripheral hypoattenuating area.

Discussion

The reticuloendothelial function in HCC differs according to the degree of differentiation. The number of reticuloendothelial cells in HCC has been reported to be lower in the less differentiated HCC (Sugihara et al., 1990; Tanaka et al., 1996). In this study, though the enhancement index tended to increase as the grade of malignancy increased, no statistical significance was verified because of a considerable overlap. We previously reported a correlation between the enhancement of tumor-liver contrast after CSIC administration and the histologic grade of HCC (Suto et al., 1995). In the present study, the mean diameter of the moderately- or poorly-differentiated HCCs was small in comparison

F

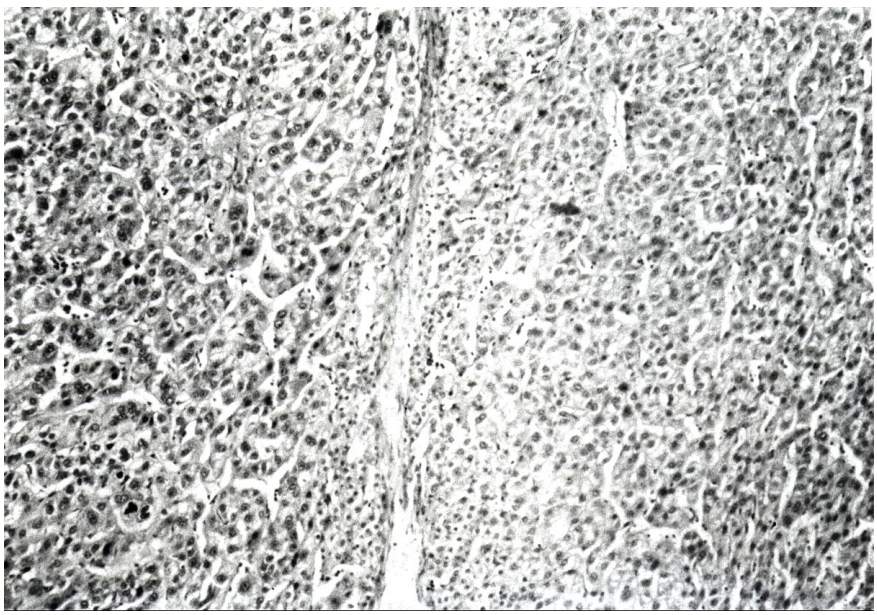

Legends to Fig. 3F: p. 120

with the previous study. The disagreement between the two studies is at least partially related to partial volume effects due to the respiratory movements during image acquisition (Butts et al., 1995). Fast T2-weighted imaging as currently offered on new scanners (Rydberg et al., 1995) can overcome this problem and one can expect that in reality the correlation between CSIC uptake and the degree of differentiation must be better than the correlation found in this study.

Three of the 21 HCCs were negative for the enhancement index. Such lesions may be indistinguishable from adenomatous hyperplasia, which has negative contrast enhancement because of the presence of reticuloendothelial cells (Suto et al., 1993). The number of Kupffer cells in 20 to 25% of moderately- or poorly-differentiated HCCs is equal to that in noncancerous tissue (Tanaka et al,. 1996). The decrease in reticuloendothelial function demonstrated by CSIC-enhanced MR imaging indicates merely one aspect of differentiation of HCC. It seems difficult to assess the histologic grade of HCC precisely by the enhancement index alone. The additional use of precontrast signal intensity and morphologic features (e.g., capsule and mosaic pattern) must also be taken into consideration (Kadoya et al., 1992).

The hemodynamic findings on CTAP and CT arteriography were reported to be correlated with the histologic grade of HCCs. The intranodular portal blood flow tends to decrease as the grade of malignancy increases (Matsui et al., 1991). The intranodular arterial and portal blood supplies have been reported to be reciprocal (Matsui et al., 1991). The intermediate lesions ranging from adenomatous hyperplasia to well-differentiated HCCs tend to have progressively less intranodular portal blood supply as the grade of malignancy increases (Matsui et al., 1991). Takayasu and colleagues, however, recently reported that the relationship between the hemodynamic characteristics and the degree of dedifferentiation of HCC could not be verified in well-differentiated HCCs (Takayasu et al., 1995).

The enhancement index correlated with the intranodular blood supply on both CTAP and CT arteriography rather than the histologic grade. The CT findings may be biased as well because of partial volume averaging. The loss of contrast in small lesions may be the reason why the enhancement index correlated with the findings of CTAP and CT arteriography rather than the histologic grade.

In contrast to CTAP and CT arteriography, CSIC-enhanced MR imaging is a noninvasive procedure. In patients with marked portosystemic shunt and/or laminal flow of contrast material, we found difficulty in assessing the intranodular portal blood supply. The hemodynamic evaluation of lesions within the wedge-shaped portal flow defect or arterioportal shunt was difficult. CSIC-enhanced MR imaging was unaffected by portal flow abnormalities (Kamba et al., 1994). Spin echo imaging, which we have used, is inferior to CTAP and CT arteriography in detecting small lesions less than 1 cm in diameter because of its lower spacial resolution (Kamba et al., 1994). High resolution imaging by fast T2-weighted spin echo sequences (Semelka et al., 1993) can overcome this problem.

CSIC-enhanced MR imaging allowed noninvasive evaluation of the intranodular reticuloendothelial function. The findings of CSIC-enhanced MR imaging correlated with the hemodynamic findings on CTAP and CT arteriography. We consider this procedure as a supplementary method for evaluation of the histologic grade of HCC prior to performing invasive procedures such as angiography and biopsy.

References

1 Butts K, Riederer SJ, Ehman RL. The effect of respiration on the contrast and sharpness of liver lesions in MRI. Magn Reson Med 1995;33:1–7.
2 Kadoya M, Matsui O, Takashima T, Nonomura A. Hepatocellular carcinoma: correlation of MR imaging and histopathologic findings. Radiology 1992;183:819–825.
3 Kalender WA, Seissler W, Klotz E, Vock P. Spiral volumetric CT with single-breath-hold technique, continuous transport, and continuous scanner rotation. Radiology 1990;176:181–183.
4 Kamba M, Suto Y, Kato T. Chondroitin sulfate iron colloid-enhanced MR imaging in patients

with hepatocellular carcinoma: comparison with CT during arterial portography. Acta Radiol 1994;35:570–575.
5 Kamba M, Suto Y, Kodama F, Ohta Y, Kobayashi J, Horie Y, et al. Hepatocellular carcinoma exhibiting a concentric structure of different histologic grades: evaluation by chondroitin sulfate iron colloid-enhanced MR imaging. J Magn Reson Imaging 1996;6:406–408.
6 Kato T, Suto Y, Matsuo T. Chondroitin sulfate iron colloid as an MR contrast agent for the hepatic reticuloendothelial system. J Comput Assist Tomogr 1993;17:603–608.
7 The Liver Cancer Study Group of Japan. The general rules for the clinical and pathological study of primary liver cancer. 3rd ed. Tokyo: Kanehara, 1992:35–36 (in Japanese).
8 Matsui O, Kadoya M, Kameyama T, Yoshikawa J, Takashima T, Nakanuma Y, et al. Benign and malignant nodules in cirrhotic livers: distinction based on blood supply. Radiology 1991;178 493–497.
9 Okuhata Y. An experimental study on MR lymphography with various iron colloid agents. Nippon Igaku Hoshasen Gakkai Zasshi 1992; 52:1148–1160 (in Japanese with English abstract).
10 Rydberg JN, Lomas DJ, Coakley KJ, Hough DM, Ehman RL, Riederer SJ. Comparison of breath-hold fast spin-echo and conventional spin-echo pulse sequences for T2-weighted MR imaging of liver lesions. Radiology 1995;194:431–437.
11 Semelka RC, Shoenut JP, Kroeker RM. T2-weighted MR imaging of focal hepatic lesions: comparison of various RARE and Fat-suppressed spin-echo sequences. J Magn Reson Imaging 1993;3:323–327.
12 Sugihara S, Nakashima O, Kiyomatsu K, Edamitsu O, Kojiro M. Pathomorphologic study on macrophages in hepatocellular carcinoma. Kanzo 1990;31:12–18 (in Japanese with English abstract).
13 Suto Y, Kato T, Matsuo T, Kamba M, Shimatani Y, Ohuchi Y, et al. Chondroitin sulfate iron colloid as MR contrast agent in differentiation between hepatocellular carcinoma and adenomatous hyperplasia. Acta Radiol 1993;34:226–229.
14 Suto Y, Kodama F, Kamba M, Ohta Y. Correlation between chondroitin sulfate iron colloid-enhanced MR imaging and the histological grade of hepatocellular carcinoma. Acta Radiol 1995;36:102–105.
15 Takayasu K, Muramatsu Y, Furukawa H, Wakao F, Moriyama N, Takayama T, et al. Early hepatocellular carcinoma: appearance at CT during arterial portography and CT arteriography with pathologic correlation. Radiology 1995;194: 101–105.
16 Tanaka M, Nakashima O, Fukukura Y, Wada Y, Kage M, Kojiro M. Pathomorphological study of Kupffer cells in hepatocellular carcinoma and hyperplastic nodular lesions in the liver. Hepatology 1996;24:807–812.

(Received April 21, Accepted June 4, 1997)